5-1-2003

Development of an Active Tether

Eric Barta
Trinity University

Chris Kruzel
Trinity University

Mason McIntire
Trinity University

Laura Wille
Trinity University

Development of an Active Tether

Senior Design May 1, 2003

Group Members:
Eric Barta
Chris Kruzel
Mason McIntire
Laura Wille

Group Advisor: Dr. Kevin Nickels

Trinity University
San Antonio, TX

Abstract:

The purpose of this text is to describe the design and testing of an active tether capable of assisting a search and rescue robot. In order to communicate with the robot in a search and rescue environment a tether is a viable option to transmit power, control, and even life support for victims to the robot. However, applying the tether in this environment opens the robot to new obstacles involving this support. The tether is capable of snagging itself on multiple contact points in the search and rescue zone that can ultimately hinder the robot from moving further. The goal of this project is to develop an addition to this tether to avoid these issues.

A biologically inspired design was chosen for this purpose that mimics the cilia found on microorganisms and in the human esophagus. The theory behind this is that by surrounding the tether in multiple cilia the tether will be pushed away from any corner that could cause a snag. The development of a cilia design outlined in this paper provides inspiration for further research, but does not generate a viable solution to the stated problem.

Executive Summary

This report is a detailed analysis of the entire Active Tether project. The report contains information on all aspects of the project ranging from testing equipment to the final analysis of our design. This is a brief overview of the entire report.

The inspiration for this project comes from the use of search and rescue robots in the World Trade Center disaster. Search and Rescue robots communicate through either a tether or wireless communication. There are a limited number of frequencies that wireless communication can operate on, and rescue workers must use a large number of these to communicate with each other. Therefore, most robots use a tether to communicate through. Since the tether is a hindrance on the effectiveness of the robot, the design problem is to produce a method of reducing this hindrance as much as possible.

Our design must prove to be more effective than the passive tether in a series of tests. These tests will measure the amount of drag that is placed on the robot. When the drag is higher than the pulling power of the robot, the robot becomes stuck. To measure this drag force we will use a data acquisition system that will measure the strain placed on the mounting bracket between the tether and robot. We will run a series of four (4) tests using cinder blocks to simulate a 90° turn, a 180° turn, an s-curve, and a narrow opening between cinder-blocks.

Two initial prototypes were constructed. The first prototype is the wheeled design, which is discussed in more detail in section 3.1. The wheeled design consists of four (4) evenly spaced powered wheels around a PVC pipe. The purpose of this design is to move the tether at the same speed of the robot. This concept would essentially reduce almost all drag placed on the robot. However, due to the size of the motor used to power the four (4) wheels, the design became too large and bulky. Moreover, the drive shaft used to power the four (4) wheels also failed because the maximum bending radius of the shaft is larger than the radius of the PVC.

The second initial prototype was the relief section design. This design can be seen in more detail in section 3.2. The purpose of this design is to pull the tether forward, while not hindering the forward motion of the robot. The design uses a winch motor connected to two rigid sections. These sections are connected with flexible tubing. When the motor is engaged, the winch will pull the trailing section forward, thus producing overall forward motion of the tether. This forward motion will also result in the reduction of drag placed on the robot. However, again with the size of the motor, the design became too large.

Having learned that the size of the design is an important factor, we decided to implement an additional set of criteria to which the final design must adhere. The final design is inspired by the biological phenomenon cilia. Cilia are meant to propagate motion to the cell. The final design uses this idea to reduce the drag placed on the robot. The design consists of five (5) short aluminum rods even spaced around a ring of PVC. The rods will reduce the drag placed on the robot because the obstacles will slide along the aluminum rods rather than dig into the tether.

The results of our testing (section 5) shows that the cilia design effectively reduces drag placed on the robot in both the 180° test, and the narrow opening. However, the tether increased drag in the 90°, and s-curve tests. In conclusion, it is felt that the concept of actuating a tether to assist a robot through the search and rescue environment is valid. The final design of this text; however, does not necessarily overcome the expected rigors of the 'hot zone' environment

Table of Contents

1 Introduction

The collapse of the World Trade Centers on September 11, 2001 presented a unique opportunity to evaluate the effectiveness of several search and rescue robots. Robots developed for this purpose had only limited success in their attempts to traverse the hot zone of the collapsed buildings. The hot zone environment consists of confined spaces such as the inside of a collapsed building and is often littered with debris, dust, and water. One significant limitation of these robots was their ability to communicate with the rescue personnel at the base station while pushing into the hot zone.

In the hot zone of a disaster area the metal and concrete likely surrounding the robot makes wireless communication of audio and video signals difficult. In addition to interference from debris, there is an immense amount of rescue equipment and emergency personnel with wireless communication devices occupying available radio frequencies. One alternative to wireless communication is the use of wired communication via a tether. Using a tether allows for audio, video, and power signals to be clearly transmitted as well as for rescue materials such as air and water to be transported from the robot operator to the robot in the hot zone. However, placing a tether between the robot and a base station creates significant problems. The tether often gets caught in the rubble and restricts the progress of the robot. Using a tether limits the range and mobility of the attached robot. This makes search and rescue robots less effective in saving lives.

The purpose of this project was to design and build a tether that can attach to a search and rescue robot. The following is a list of criteria that must be met for the project to be successful:

1. The design must reduce the drag placed by the tether on the robot in the harsh setting of a hot zone environment.
2. The tether must protect its payload from reasonable environmental hazards of the hot zone.
3. The tether must be transportable and storable.
4. The tether must be long enough to demonstrate the effectiveness of an active tether design versus a passive tether design.

The success of the active tether project will be evaluated on the accomplishment of the above stated criteria as well as the following design metrics. The following design attributes will provide a means of evaluating designs and suggesting design improvements. The effectiveness of the tether to satisfy each

of the evaluation criteria will be determined through a series of tests designed to isolate each criterion. The drag placed on the robot by the tether compared to a passive tether must be reduced by 10% in a simulated hot zone environment. The tether flexibility and maneuverability must not hinder the operation of the robot. Thus, the tether must be able to maneuver around a 90 degree turn, a 180 degree turn, S-curve, and straight crevasse. Moreover, the design must assist the tether in enduring harsh environments, including water, heat, and rough surfaces. The design must be built to accommodate various possible payloads, all of which may have a diameter of up to ¾ inch. A major concern for the design will be power consumption. Due to the nature of the problem, and the limited power supply at a test site, the design cannot consume a large portion of the power supplied to the robot. Lastly, the cost of our design must not exceed $1000.00.

2 Testing Equipment

The problem statement of the design asks for a 10% reduction in drag in a simulated hot zone environment. To measure this, an obstacle course is made to see how the tethers perform in the real-world setting.

2.1 Obstacle Course

In the obstacle course testing, the drag force each prototype creates on the robot can be measured. Excessive drag is a negative attribute since our designs are ultimately trying to reduce this attribute. Cinder blocks were selected to simulate the desired turns and bends possibly found in a hot zone environment. A picture of this test bed can be seen in Appendix A.1. The obstacles simulated the problems outlined in our problem statement and are shown in Appendix A.2.

The testing will consist of three components: the robot, the tether, and the data acquisition equipment, as shown in Appendix A.1. The robot will be simulated by an RC car that was provided by the Trinity Engineering department. The car has been tested to find that it has a pulling power of 3 lbs force. A digital 'fish-scale' was used to measure this value. The tether that will be used is a ½ diameter power cable that is cut to 9 ft. This cable will be attached to the rear of the car with an aluminum L-bracket, and fastened with two hose clamps on either side of the L-bracket. Figure 2.1.a shows a model of the RC car with the tether attached.

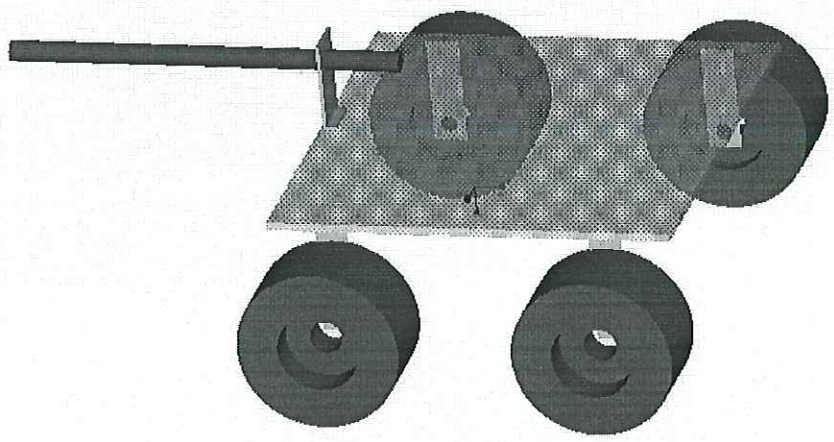

Figure 2.1.a, Testing Physical Set-up

2.2 Data Acquisition Equipment

The third component of the testing is the data acquisition equipment. The equipment is separated into four parts: the strain gauges, the Wheatstone Bridge, the datalogger and the instrumentation amplifier. The L-bracket on the RC car begins to bend in response to strain placed by the tether on the robot. The strain gauges on the L-bracket will change their resistances in response to strain. In turn these resistances will be changed into voltage differences by the Wheatstone Bridge, amplified, and sent to the datalogger. The final voltages will represent the strain placed on the RC car by the tether.

2.2.1 Wheatstone, Strain Gauges, and L-Bracket

In selecting strain gauges for our aluminum L-bracket, it was first necessary to predict the bending strain that our L-bracket will see. Calculating this strain using the quotient of stress divided by the modulus of aluminum, it was possible to predict such a strain. The calculations for this model can be seen in Appendix B.1. Predicted values of this prediction are shown in Appendix B.2. With a range of weights from 0 g to 2 kg, a roughly predicted range of strain was between 0 and .432 με.

The strain gauges that were found in house have a gauge factor (G) of 2. With such a small value it was important to choose a strain gauge configuration that would maximize their sensitivity to the bending moment of the drag force. The four gauge set-up was chosen for this purpose. This created a 482%

improvement over the simple single strain gauge application when using a 9 V excitation voltage (Vex). The selection table for this can be seen in Table 2.2.1.a.

Table 2.2.1.a: Bridge Selection Table {2}

Orientation	# of Gauges	Voltage vs. Strain Relationships	Maximum Expected Voltage (Vo)	% change
One on tension side	1	$Vo = -\frac{1}{2}\left[\frac{1}{1+\varepsilon G/2} - 1\right] Vex$	1.408	0 %
One in tension another in compression	2	$Vo = \frac{-G\varepsilon}{2} Vex$	4.099	191.09 %
Two in tension and two in compression	4	$Vo = -G\varepsilon \bullet Vex$	8.198	482.18 %

There are additional benefits to this selection on top of the added sensitivity. The most important of these is the nulling of any temperature ambiguities between the strain gauges. When using only one or two strain gauges, it is necessary to use three or two standard resistors respectively in the remaining four-resistor set-up of the Wheatstone bridge{2}. Doing so allows the possibility that temperature differences between the resistors and the strain gauges could affect their resistances.

To measure the voltage change in these four strain gauges it is necessary to place them in a Wheatstone bridge configuration. The design for this component can be seen in Figure 2.2.1.a.

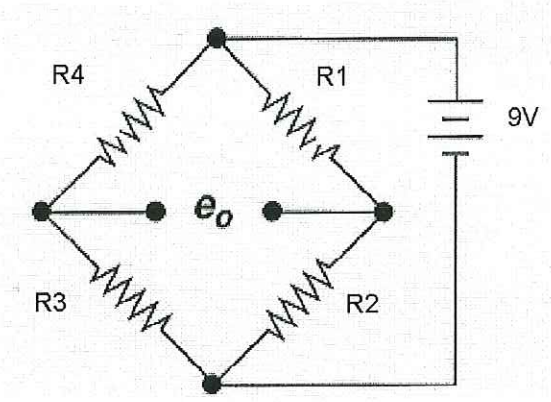

Figure 2.2.1.a: Wheatstone Bridge

In this configuration there are two strain gauges that are placed in tension on the L-bracket and two in compression. For our design resistors R1 and R3 are in tension while R2 and R4 are in compression. An excitation voltage is applied using a nine volt battery. A drawing of the final design of the four resistors and the L-bracket can be seen in Figure 2.2.1.b.

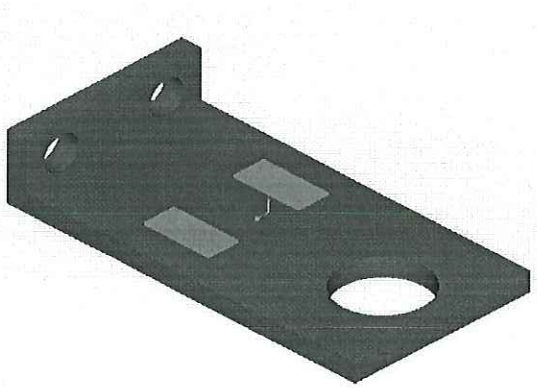

Figure 2.2.1.b: L-bracket Final Design

In this drawing there are also two strain gauges on the underside of the L-bracket that cannot be seen, which were referred to as resistors R2 and R4 in the Wheatstone setup.

To check for proper operation of the Wheatstone bridge, a series of weights ranging from 0 to 2000 g were hung from the L-bracket. As each weight was applied a digital multimeter was used to measure the Wheatstone's output voltage, labeled e_o in Figure 2.2.1.a. Due to the fluctuation in these measurements, the accuracy is a tenth of a millivolt. Three tests were done and the plot of their averages can be seen in Figure 2.2.1.c. Also on this plot are the 95% confidence intervals of these means represented by the error bars.

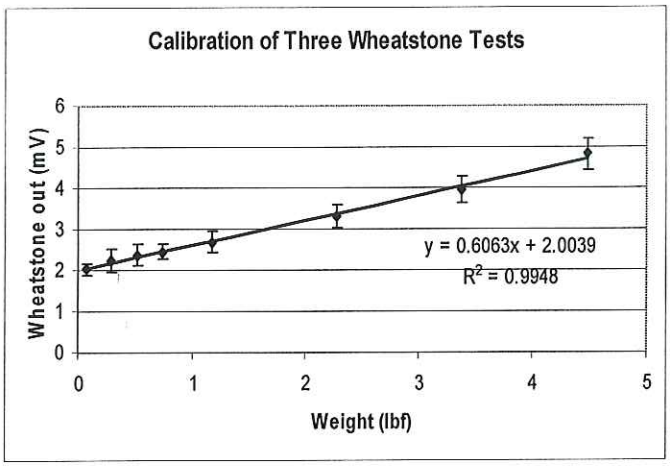

Figure 2.2.1.c: Wheatstone Calibration Plot

The strong linear relationship the four-gauge method provides is clear from Figure 2.2.1.c.

2.2.2 Quadvolt Datalogger

The data logger is needed to store the voltages from the data acquisition (DAQ) unit over the course of our experiment. The chosen module can record and store voltages in real-time. These measurements can later be downloaded and plotted on the computer. It has its own software on which to graph the data and send it to Excel. This will be used to record the voltages (which represent the strain) for the tests. The time increments will be set prior to the testing. The smallest time increments are 1 second apart. Additionally, the datalogger has a resolution of a half a millivolt and a range of measurement from –1 Vdc to 16 Vdc. These ranges are important to note considering the small voltages from the strain gauge shown in Figure 2.2.1.c.

2.2.3 Instrumentation Amplifier

The final component of the signal-conditioning unit is the instrumentation amplifier. First, it is necessary to amplify the signal out of the Wheatstone bridge because of its small magnitude. As seen in Figure 2.2.1.c, the maximum voltage from our Wheatstone is 4.7 mV. The chosen data logger is known to have a resolution of .5 mV and a range of -1 to 16 V. Knowing this, it is possible to choose a suitable gain to amplify the signal before the data logger.

An instrumentation amplifier was chosen because of its unique advantages over traditional operational amplifiers. The instrumentation amplifier has a differential gain. That is, the difference between the two Wheatstone bridge outputs is amplified and ideally is centered on 0. Also, the instrumentation amplifier has an internal feedback resistor network that is isolated from its signal input terminals. The gain can be changed by adding an external resistor. We are using the AD620, a classic monolithic dual-input instrumentation amplifier from Analog Devices. This goes in the circuit as seen in Figure 2.2.3.a.

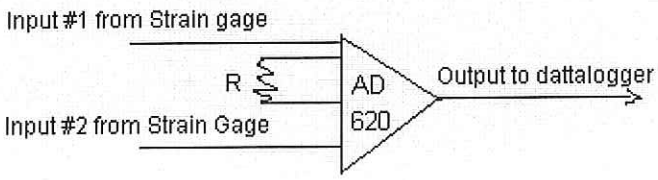

Figure 2.2.3.a: Instrumentation Amplifier{3}

This can handle gains from 1 to 10,000. The equation for the gain is{3}

$$Gain = \frac{49400\Omega + 1}{R} + 1 \qquad (2.2.3.i)$$

Here R is the external resistor. Since the data logger has a limited resolution, the larger the amplification the better. Excitation voltages of positive and negative nine volts were used to power the instrumentation amplifier. Equation (2.2.3.i) accounts for an excitation voltage around 15 V to be used, equation (2.2.3.ii) was calibrated for our particular setup:

$$Gain = \frac{47488.2\Omega + 1}{R} + 1. \qquad (2.2.3.ii)$$

To obtain an increase in magnitude, a 47.3 Ω resistor was chosen. Having a gain of 1000 $^{V}/_{V}$, a maximum voltage around 4.7 V can be expected.

2.3 Final Data Acquisition Design

The completed schematic, shown in Figure 2.3.a, incorporates the Wheatstone bridge, instrumentation amplifier, and output to the datalogger.

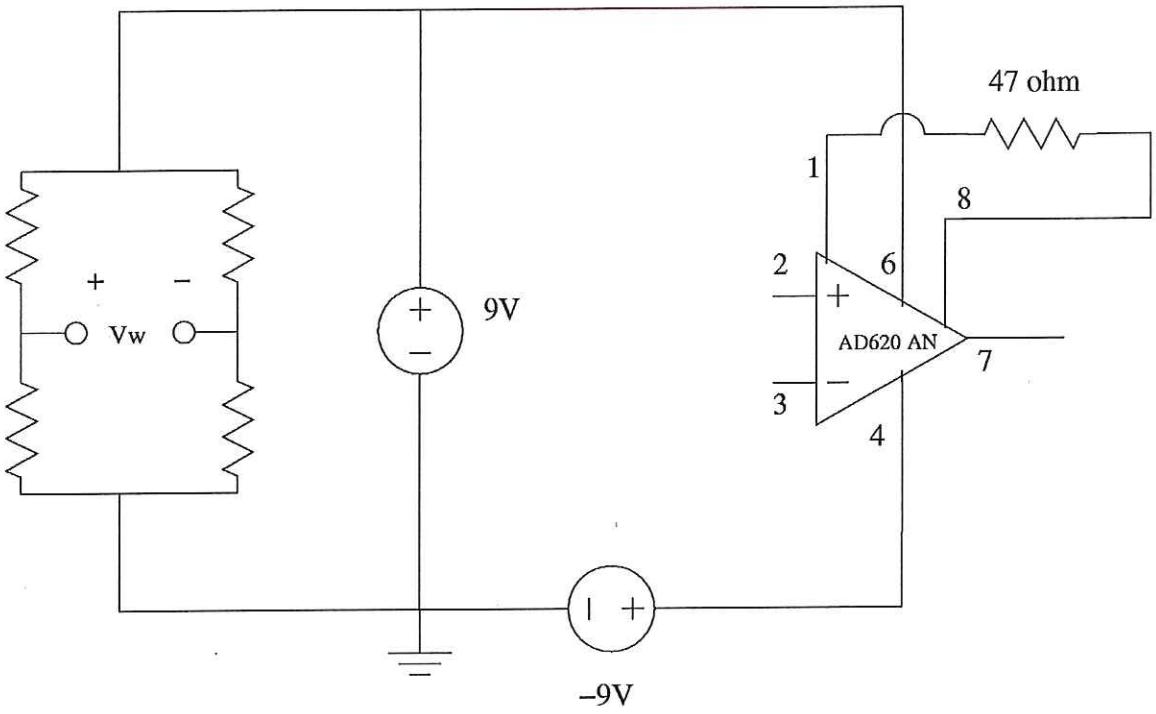

Figure 2.3.a: Final Schematic of Data Acquisition Circuit

To calibrate this entire circuit, varying weights were applied to the L bracket as previously described. Voltage readings were taken from the datalogger running real time on the computer. Six trials of this setup were completed. The means of these trials gave the plot in Figure 2.3.b.

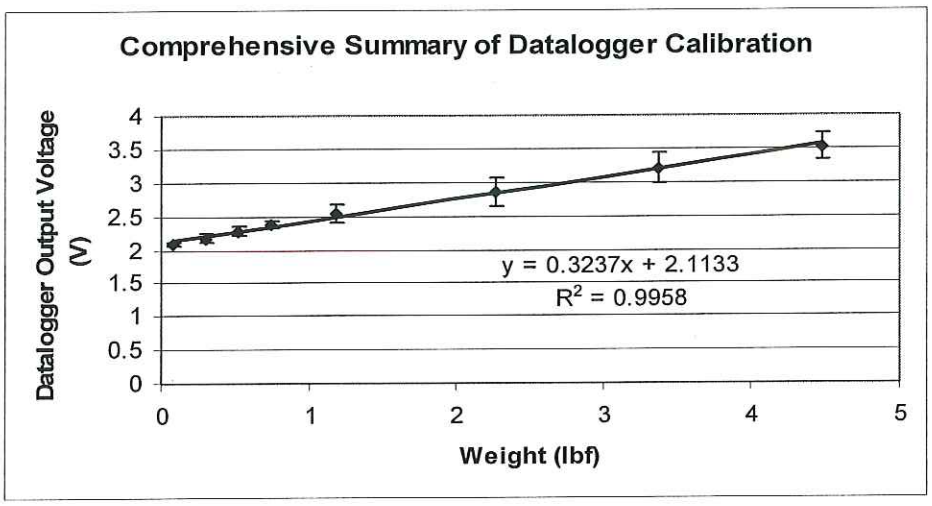

Figure 2.3.b: Calibration Curve for Datalogger and Completed DAQ

The error bars on this plot represent the 95% confidence interval of each individual sample weight. Using the calibration equation it was found that the measured weight varies on average .37 Lbf. This variation is acceptable for our application.

The datalogger is rated as having a resolution of 0.5 mV. Using the calculated calibration curve in Figure 2.3.b, it is calculated that the setup can measure changes in weight as low as .002 Lbf. This is acceptable for our application.

3 Initial Prototypes

The initial designs for the active tether came from a wide variety of inspirations. Some were biologically inspired while others were just imaginative. The designs were broken into two possible solutions, preventative and more active 'problem solving' measures. The latter methods use forms of actuation to either drive the tether along with the robot or maneuver obstacles. Two initial prototypes using these theories were designed and built forming the wheeled design and the relief section design.

3.1 Wheeled Design

The idea behind the wheeled section design is to provide power for the tether to drive around obstacles and alleviate the drag force created by the passive tether. To do this, an 11 in section of PVC with

a diameter of 4.5 in was mounted with four wheels. The wheels were equidistant around the cylinder and powered by a DC motor capable of .115 in lbs. The wheels were powered consecutively from the motor using a subminiature flexible drive shaft. The schematic of this design can be seen in Figure 3.1.0.a.

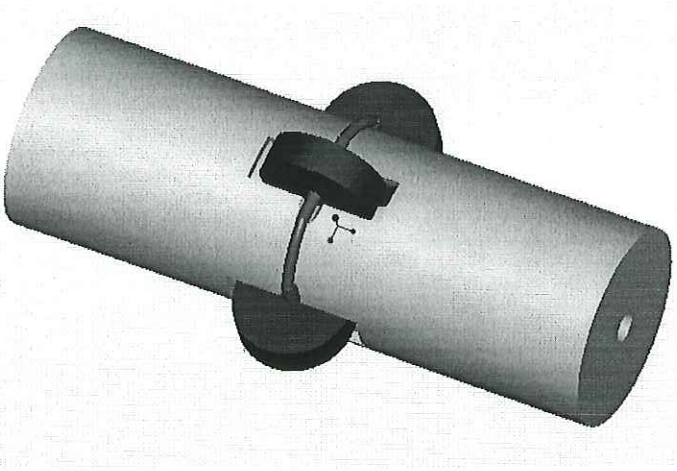

Figure 3.1.0.a: Wheeled Design Schematic

3.1.1 Wheeled Design Testing

The wheeled design was tested using the obstacle course discussed in Section 2.1 and Appendix A. Testing of this design was not capable however due to a failure in the subminiature drive shafts. Since the wheels were not able to turn, then the testing of this design was inconclusive of the possibilities of the wheeled design.

3.1.2 Drive Shaft Failure Analysis

As mentioned above, a subminiature flexible drive shaft was used to transmit power from the motor to the four wheels of the Powered Wheel design. Upon testing of the prototype it was discovered that the drive shaft was incapable of transmitting power to the wheels of the design. This section will briefly explain why the implementation of the flexible drive shafts was unsuccessful.

The PVC housing of the prototype has an outer radius of 2.025 inches. The drive shaft that was selected and implemented in the design has a minimum bend radius of 2.50 inches. Because the drive shaft was run along the outside of the PVC housing, it is clear that the design did not satisfy the 2.5 inch minimum bend radius of the drive shaft.

The flexible drive shaft used in this construction is not a bi-directional drive shaft. The drive shaft is essentially a long coiled wire that is free to rotate around a core shaft. When the shaft is turned in one direction, the force translates through the coils and into the coupled wheel. When the drive shaft is turned in the opposite direction, the force is not translated through the shaft, but rather the force causes the wire to uncoil from around the shaft. In this orientation, translation of power is dramatically less efficient. One major problem with the construction of the powered wheel prototype is that the drive shafts were not uniformly oriented, meaning that some were oriented for clockwise rotation and others for counter-clockwise rotation. This led to a buckling effect, which translated power from the motor into the coils of the drive shaft rather than through the drive shaft and into the wheels. Adding to the buckling effect of the drive shafts was the friction generated between the brackets holding the shaft onto the PVC shell and the coupled axles. A rough connection was created using JB Weld, an epoxy-like material. Each connection joined a rigid axle section to a flexible section. A major source of failure in the connection technique is that the flexible shafts were not perfectly aligned with the solid axles. This imbalance likely caused a significant loss in torque and was an additional source of resistance in the drive train.

It is clear from this analysis of the flexible drive shaft that this was not an appropriate use of the material. The many implementation problems noted in this paper are avoidable if a more careful construction process is carried out; however, the minimum bend radius and the joint connection difficulties are design problems that cannot be overcome with careful construction.

3.1.3 Wheeled Section Prototype Lessons Learned

When analyzing the failure of this design, many things were cleared up about the prototype's design. It is clear that our application of the subminiature drive shafts was wrong and perhaps mislead. It was concluded that these shafts could not be used to fulfill our design.

In addition to the drive shafts, wheel spacing was a possible source of problems. It was clear when pushing the PVC under our own power across the table that two wheels were not always touching the contact surface. It is now believed that an arrangement of five wheels rather than four would be better. Implementing such a design would further increase the complexity of construction in this design and overall size.

Ultimately this design showed the ineffectiveness of using a motor to power the tether. Considering our particular resources, the addition of a motor to the tether would require a large housing. Such a large housing is adverse to our goal in helping the maneuverability of the design.

3.2 Relief Section Prototype Design

The relief section concept is based on the hypothesis that adding power to the tether at regularly spaced intervals will generate the force necessary to maintain the forward progress of a search and rescue robot. In the design, the relief sections are made from expandable tubing. This tubing is capable of stretching under the initial force of the hindered tether as it encounters an obstacle. Allowing this section to deform during a snag was intended to prevent the halting of the robot. The passive prevention was intended to delay the effect of a snag long enough for the snag to be overcome by a series of winches between the sections. A schematic of the relief section prototype design is shown in Figure 3.1.1.a.

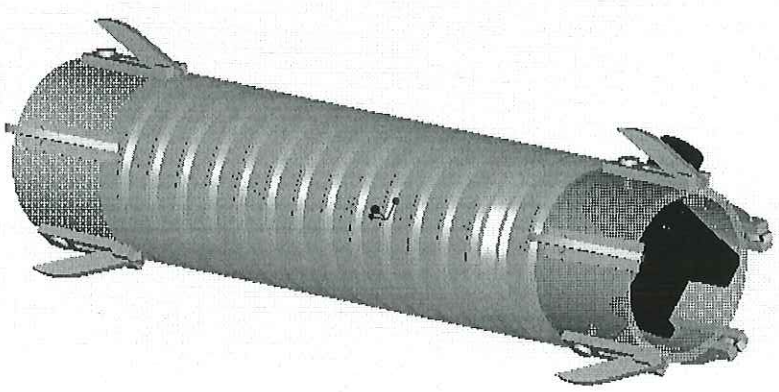

Figure 3.1.1.a: Relief Section Prototype

The series of spikes shown in Figure 3.1.1.a were intended to provide friction between the tether and the ground when the tether was snagged. The spikes are spring loaded, which allows them to extend when there is no weight on them and to fold down when they are in contact with the ground or an obstacle. The motor was the source of power that retracted the passive section of the tether back into a non-extended position. The force generated by the motor pulled the expandable section of the design forward while at the same time pulling the trailing section of the tether.

The prototype was controlled by a hand held controller, which could make the motor rotate in the forward and reverse directions. The controller was used during testing of the prototype to expand and contract the expandable sections of the design.

3.2.1 Relief Section Prototype Testing

Once the design was assembled and the motor was successfully retracting the trailing sections, it was run through the series of tests described in Section 2.1.0 and Appendix A of this report. The first test that was conducted on the relief section prototype was the 90° test, shown in Appendix A. The test was aborted when the design was not capable of making it around the corner of the cinder block. Drag data was collected from this test, but it is not significant because the test was not successfully completed.

The cause of failure in this first test was easily determined. The leading edge of the motor housing is rigid and blunt, thus there is no ability for this section to advance past the cinder block when it becomes caught. The spikes were intended to prevent this from occurring, but were spaced too far apart for this to be successful. Additionally, the diameter of the completed prototype was 6 inches. The large diameter of the design allowed for large region of contact between the tether and the cinder block.

3.2.2 Relief Section Prototype Lessons Learned

The negative results of the relief section prototype testing implied that several new design constraints would be necessary for a design capable of meeting the objectives described in the projects problem statement. Most importantly, it was determined that a successful design could not incorporate a motor. The large size and awkward mounting positions of a motor created a design that was too large and bulky for success. Additionally, it was determined that a successful design would need to have a smooth sheathing material that did not contain rigid section longer than 2 inches.

4 Final Prototype

Using the lessons learned in the two prototypes, it was decided that the best choice would be to move in a completely different direction. The initial active 'problem solving' methods were unsuccessful in maintaining the small profile of the original passive tether. In our problem statement it was envisioned that the design would not hinder the movement of the robot and should therefore be considerably smaller than the robot itself.

Respecting this ideology, it was chosen to continue with the preventative method of actuating the tether. This method would not require the application of a motor to the design and would considerably reduce its size. A design idea discussed in the brainstorming of alternative designs was chosen to achieve these results.

New criteria were added to the problem statement given in section 1 to address the shortcomings of earlier design specifications and lessons learned in the previous two designs. The design cannot have a diameter greater than 2 inch, no less than 3 inches between rigid sections, and the length of any rigid sections cannot be larger than 1 inch. It is believed that such constraints will keep the overall diameter of the design down and keep the flexible integrity of the original passive tether.

4.1 Cilia Design

The purpose of the cilia design is to reduce the drag placed on the robot. A sequence of cilia-like rods surrounds the tether diverting it around any obstacles. The cilia design is shown in Figure 4.1.0.a.

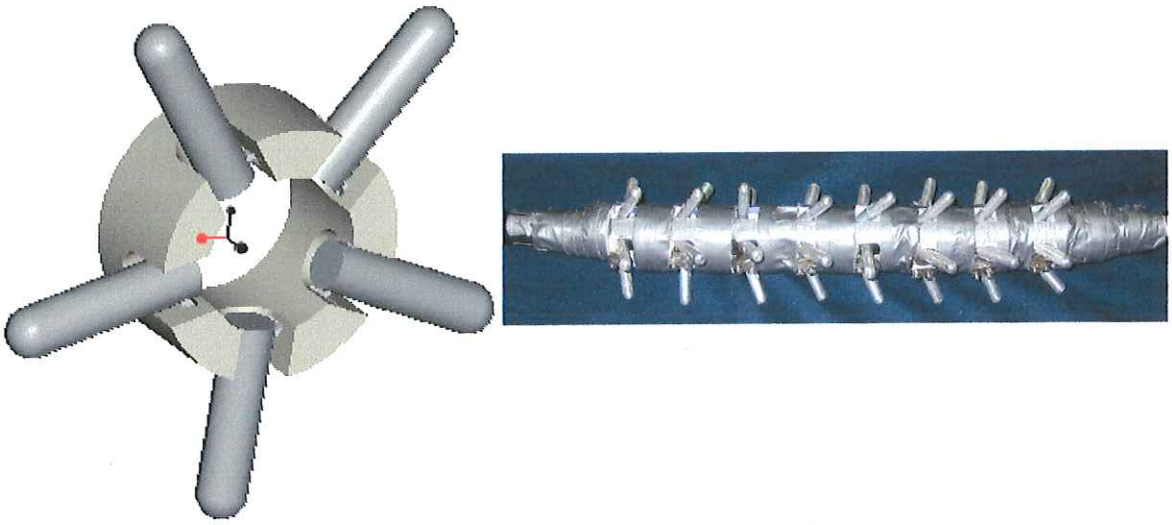

Figure 4.1.0.a: Cilia Design Schematic and Picture

Each section of the cilia design was constructed from two pieces of PVC. The inner piece is a $^{7}/_{8}$ in diameter PVC, which will have notches cut in the front at a 45 degree angle to allow for the five cilia. The cilia are made of ¼ inch aluminum rods cut to a length of 1 inch. Moreover, the inner piece will have a groove placed into the outer surface that is $^{1}/_{16}$ inch deep and $^{3}/_{32}$ inch wide. This groove will allow for a cable to anchor each cilium in place. The outer PVC piece will have an inner diameter of $^{7}/_{8}$ inch, and will

slide over the smaller PVC. The outer PVC will have the same notches cut into it to allow for the five cilium, and will enclose the cable in the groove. The length of each PVC section will be $^{5}/_{8}$ inch.

Each individual cilium was constructed from aluminum rods, which have a low coefficient of friction against hard surfaces that will generally be found in the testing environment. Furthermore, the rods will be attached to the design using a type 304 stainless steel cable, which has a $^{1}/_{16}$ inch diameter that is placed in the groove fashioned into the inner PVC pipe. Five cilia have been chosen due to the geometry of the PVC and lessons learned in the previous two designs. When using five cilia, there is sufficient space between each cilium to allow for easy construction, as well as keeping any obstacle away from the surface of the tether. There is a clearance of at least 0.2 inches between the tip of the cilium and the surface of the PVC. This calculation is done with the cilium placed at the maximum forward motion position of 45 degrees. These calculations can be seen in Appendix C.1. Additionally, at this position, expected loads were calculated and can be seen in Appendix C.2. The expected maximum load at a cilia position of 45 degrees is 26.36 Lb_f. When the design is in forward motion, any obstacle will slide along the cilium, which has a lower coefficient of friction than the surface material of the tether, until it reaches the tip of the cilium. At this point, the obstacle will fall to the next set of cilia, and the process will repeat. Figure 4.1.0.b shows the path of an obstacle when in forward motion.

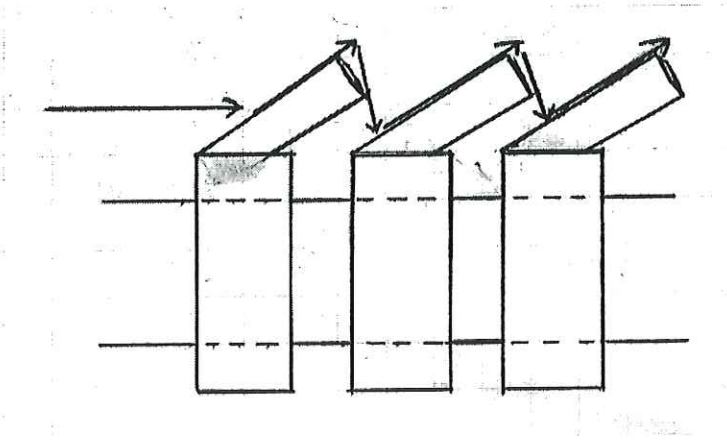

Figure 4.1.0.b: Obstacle Path in Forward Motion

However, the design also addresses the fact that the tether may be used to pull the search and rescue robot out of a hot zone. Therefore, the cilia must fold down to not hinder the reverse motion of the robot. This is achieved by fastening an elastic material to each cilium, and anchoring it to the PVC.

Therefore, when reverse motion is implemented, the cilia that make contact with any surface will fold back. Then, when forward motion is reinstated, the cilia will fold to their original 30 degree position.

4.2 Cilia Design Testing

The first phase of testing on the cilia prototype was conducted on a tether with eight cilia sections spaced 0.25 inches apart. The spacing between each section was filled with a Nomex Aramid fabric that was very flexible and compact. With the material in place, a duct tape sheathing was placed around the tether and the four tests described in Section 2 of this report were conducted. The results of the first phase of tests are shown in Table 4.2.a.

Table 4.2.a: Initial Cilia Design Testing Summary (drag force measured in Lbf)

	Active Average	Passive Average	Difference from Passive	% Diff
90	failure	13.533	N/A	N /A
180	13.386	failure	N/A	N /A
Straight	13.209	13.276	0.067	0.500
S Curve	failure	failure	- 20	N /A

The results from the first round of tests were unimpressive. As shown, half of the tests were unable to be completed, and the remaining tests yield results that do not vary from one another enough to perform a comparative analysis.

The low quality of the data recorded from the first test was believed to have been caused by two major factors that were observed during the test. First, the remote control car was not capable of generating the force needed to pull the designs through the test-bed. An additional problem with the remote control car used in the testing setup was the sudden jolt of forward motion that resulted from actuating the car with the remote. This jolt caused a spike in the force measured in the L-bracket on the car and thus the results of all tests revealed this maximum force and not necessarily the largest force caused by the tether interacting with the obstacles in the test-bed.

The second problem observed in the testing of the prototype was that the spacing between each cilia section was too great. The flexible material between each section was exposed to the obstacles when moving around a corner. This resulted in the active tether becoming stuck and a failure to be recorded for each test.

To solve the problems observed in the first phase of testing, modifications were made to both the cilia design and the test setup. The spacing between each cilia section was reduced to .0625 inch and there was no spacing material inserted into the gaps. The test setup was modified by not actuating the car with the remote control, but rather pulling it through the test bed by hand. This allowed for a smooth acceleration through each test, which eliminated the spikes in force observed during the first phase of testing.

5 Results

A second phase of testing was conducted utilizing the changes described in the previous section of this report. The changes made to the design and to the test setup were successful in generating usable data, as can be seen from the results summary shown in Table 5.a. Each test was repeated twice, and the average value of the two runs is the value shown.

Table 5.a: Testing Summary for Second Design Iteration (drag force measured in Lbf)

	Active Average	Passive Average	Difference from Passive	% Diff
90	7.329	7.039	- 0.29	- 4.12
180	12.295	13.494	1.200	8.880
Straight	5.537	9.330	3.794	40.660
S curve	FAILURE	9.723	N/A	N/A

Further testing of the criteria of mentioned in Section 1of this report was performed to determine the overall effectiveness of the Cilia Design. To test the flexibility of the Cilia Design, it was necessary to measure its bend radius. This was measured as 2.5 inches for the Cilia Design and 1.5 inches for the passive tether.

To determine the design's susceptibility to environmental hazards, it is significant that the maximum spacing between the cilia segments is $^1/_4$ inch. At the maximum bend radius of 2.5 inches, only a $^1/_4$ inch of the payload will be open to the environment. The remainder of the payload is covered in the PVC shell of the design and is thus protected from the surrounding environment.

To account for the transportability of the design, it was decided to determine the storable volume of the Cilia Design. This was calculated assuming that the design would be coiled around a one foot

diameter spool for storage. When stored in this configuration, the Cilia Design storage volume is 353% larger than the passive tether storage volume.

The final two criteria to test are the design's ability to carry a range of payloads and to not use large amounts of power from the base station. The Cilia Design has an inner diameter of .75 inches that can accommodate any payload less than or equal to that diameter. The design uses no motors or other power consuming devices and thus has no power consumption.

6 Conclusions and Recommendations

The results from Table 5.a clearly show which tests the Cilia Design had success in reducing the drag placed on the robot. An advantage in drag force was achieved in both the 180-degree and the straight tests. In these two tests the design offered an 8.8 % and 40.6 % improvement respectively over the passive tether.

From the data in Table 5.a it is believed that the cilia design would generate an advantage over the passive tether in situations where there is more than one contact point, like the 180-degree and straight tests. Additionally, the results imply that the tether would be effective in open environments void of tight curves and narrow spaces. Because tight curves and small voids are present in a hot zone environment, it is not reasonable to conclude that this design should be used on a search and rescue robot in a hot zone environment. The limited success that the cilia design had in reducing drag on the robot is significant as inspiration for further work, but does not adequately solve the specified problem.

Further success of the design can be demonstrated using the additional criteria discussed in Section 1. These criteria account for the design's flexibility, susceptibility to environmental hazards, transportability and storability, ability to carry a range of payloads, and power consumption. For flexibility, the Cilia Design reduces the overall flexibility of the tether by an inch. This added rigidity is evident from the failed S-curve test of the final design. It is understood that in order to gain the desired advantages the addition of the active tether provides, a loss in flexibility is inevitable.

When flexed at its maximum bend radius, the maximum exposed length of tether was determined in Section 5 to be $^1/_4$ inch. Accounting for the presence of rubber sheathing on the tether and this small

spacing, it is believed that there is no concern for harm to the payload by such hazards. The transportability of this design is conceivable bearing in mind the added volume of the design. Once again, it is inevitable to have an increase in this volume when discussing the addition of the active tether. The 353% increase is considered to not be large enough to hinder the search and rescue team. Finally the inner diameter of the final design is believed to be capable of housing a large variety of payloads.

In conclusion, it is felt that the concept of actuating a tether to assist a robot through the search and rescue environment is valid. The final design of this text; however, does not necessarily overcome the expected rigors of the 'hot zone' environment. Sharp turns and drops would be prevalent in the 'hot zone' environment and would pose a major problem for this Cilia Design. Despite this, the initial advantages shown in the 180 degree and straight tests show the potential benefit of an active tether system and serves as significant inspiration for further work on the concept.

Appendix A: Obstacle Course Design

Appendix A.1: Drawing of Test Bed Setup

Figure A.1.1 shows the Test Bed setup which was used for testing the designs. Aluminum rods are placed into the peg board to guide the tether in a fixed direction. The tether is attached to the RC car, and is pulled around the cinder block to test the drag placed on the robot

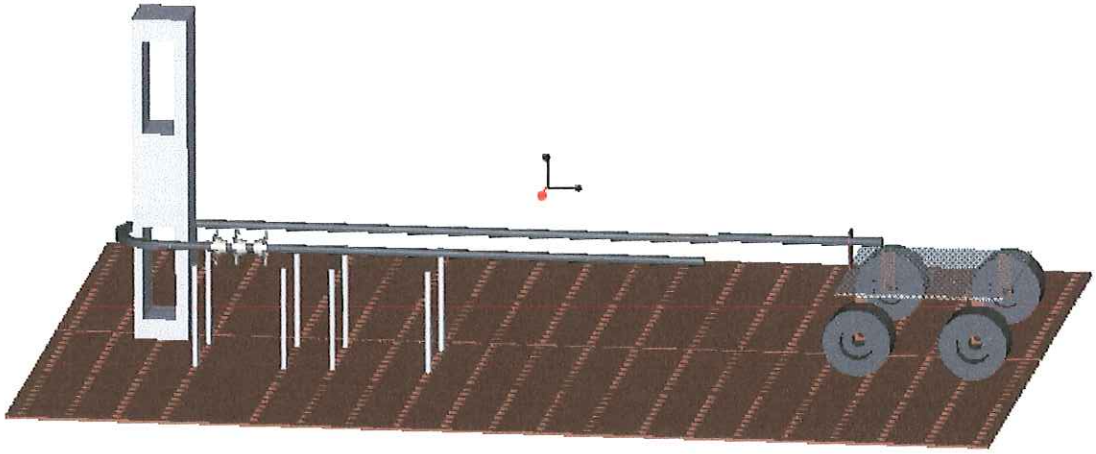

Figure A.1.a: Test Bed Setup

Appendix A.2: Arrangement of Tests for the Test Bed

Shown in Figure A.2.a are the four tests that were performed to analyze the drag placed on the robot.

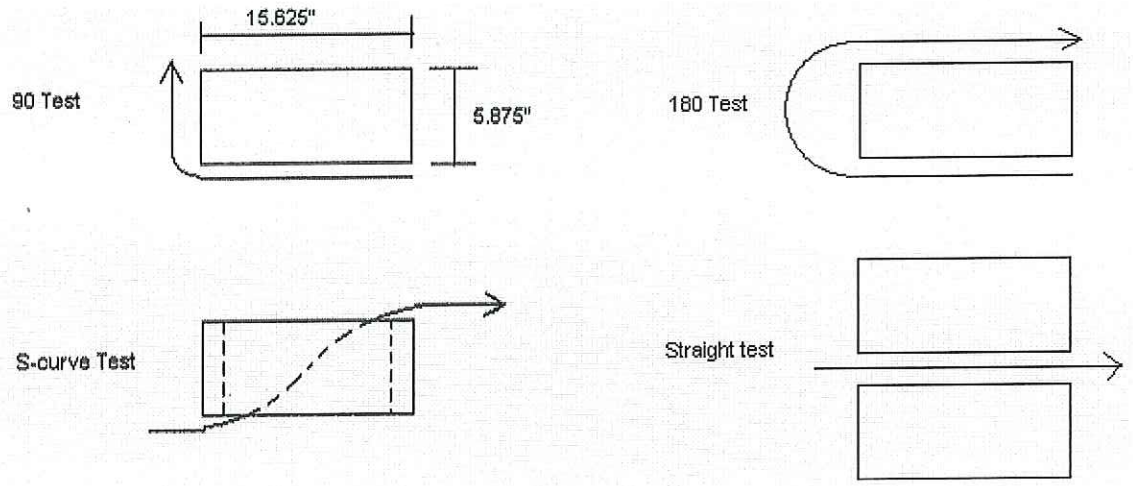

Figure A.2.a: Arrangement of the Four Tests

Appendix B: Predicted Strain Calculations

Appendix B.1: Mathematic Modeling

The following is a schematic of the load placed on the L-bracket. P signifies the load, Ac is the cross-sectional area of the L-bracket, and E is the Modulus of Elasticity for the L-bracket material.

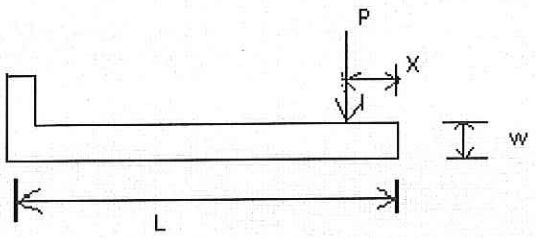

$$\varepsilon = \frac{\frac{P*(L-X)}{Ac}}{E}$$

Appendix B.2: Calculated Values

The following is a table of predicted strain in the L-bracket calculated with the shown in Appendix B.1.

	cm	m	Load (g)	Load (N)	Strain
width	3.5	0.035	0	0	0.00E+00
thickness	0.4	0.004	50	0.49	0.010792
Length from center	2.5	0.025	100	0.98	0.021585
Modulus of Elasticity		8.55E+04	150	1.47	0.032377
Total Length	6.5	0.065	200	1.96	0.04317
			250	2.45	0.053962
			300	2.94	0.064755
			350	3.43	0.075547
			400	3.92	0.086339
			450	4.41	0.097132
			500	4.9	0.107924
			550	5.39	0.118717
			600	5.88	0.129509
			650	6.37	0.140302
			700	6.86	0.151094
			750	7.35	0.161887
			800	7.84	0.172679
			850	8.33	0.183471
			900	8.82	0.194264
			950	9.31	0.205056
			1000	9.8	0.215849
			1050	10.29	0.226641
			1100	10.78	0.237434
			1150	11.27	0.248226
			1200	11.76	0.259018
			1250	12.25	0.269811
			1300	12.74	0.280603
			1350	13.23	0.291396
			1400	13.72	0.302188
			1450	14.21	0.312981
			1500	14.7	0.323773
			1550	15.19	0.334565
			1600	15.68	0.345358
			1650	16.17	0.35615
			1700	16.66	0.366943
			1750	17.15	0.377735
			1800	17.64	0.388528
			1850	18.13	0.39932
			1900	18.62	0.410113
			1950	19.11	0.420905

Appendix C: Cilia Design Calculations

Appendix C.1: Cilia Clearance Modeling

The following is a calculation of the space between the end of the rod, and the PVC shell. This gap is measured with a 30° angle. This space is measured with two rods making contact with a flat surface. X signifies the distance between the flat surface and the center of the PVC pipe.

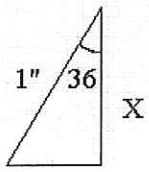

$x = \cos(36) = 0.809017$

$0.809017 - 0.5 = 0.309017$

Therefore, the clearance is 0.309017 inches.

Appendix C.2: Cilia Load Calculations

The following is a calculation for the load placed on the cable that holds the rods in place. This is done to qualify the cable selection. Moreover, the cable must have a breaking strength greater than that of the calculated load.

$$\sum M_p = L(0.62787) - N(0.23816) = 0$$
$$N = L(2.636) = 10(2.636) = 26.36lbs$$

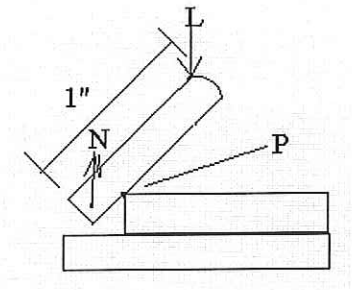

Appendix D: Users Manual for Active Tether Design

The following is a brief user manual for attaching the Active Tether attachment to your existing search and rescue robot tether. The Active Tether Design is designed to be used on any tether that has a diameter of 0.75 inches or less. It is important that after each insertion into a disaster environment each section of the tether is inspected and replaced if damaged.

Steps for Installation

1.) Slip one ring of the cilia design onto the tether and slide to the front until flush with the robot connection point.

2.) Secure the first ring to the tether with a 0.5 inch strip of duct tape.

3.) Using the 0.0625 inch spacer, position a second ring 0.0625 inches behind the first.

4.) Repeat steps 1-3, until entire length of tether is covered with the Active Tether Design.

Steps for Inspection

1.) Simply move each of the five rods on each ring to the full forward position and then to the full backwards position. If any of the rods are not free to move the full range, proceed to step 2.

2.) Remove the damaged section by removing all trailing sections. Replace all sections using the steps for instillation given at the top of this user manual.

Appendix E: Budget

Dr. Nickels' Senior Design Group (Active Tether) 2/26/2003

Description	Part #	Where From?	Price	Qty	Total
Vinyl-Laminated Nylon (width 61", thickness .022")	8810k13	McMaster	$2.88	2	$5.76
Nomex Aramid Fabric (width 45", thickness .0625")	8797k11	McMaster	$6.63	2	$13.26
Miter Gear	7297K15	McMaster	$2.59	16	$41.44
Dayton 12 VDC Permanent Magnet Gearmotor	2L011	Grainger	$28.05	1	$28.05
Model Airplane Wheels		hobby shop	$4.99	2	$9.98
Hobby Motor		hobby shop	$24.99	1	$24.99
18" Subminiature Flexible drive shaft	3135K27	McMaster	$8.09	1	$16.18
MuscleWire®		robotstore.com	$34.95	1	$34.95
pegboard		home depot			$13.78
cilia stuff (Chris)					$85.52
cilia stuff (McMaster)					$31.85
dryer venting					$7.43
					$50.00
					$363.19

Appendix F: Gantt Chart

Task Name	Duration	Start	Finish
Research and Design Specifications	31 days	Fri 8/16/02	Mon 9/30/02
Developing Alternatives	22 days	Wed 9/18/02	Fri 10/18/02
Research and Development of DAQ Hardware	125 days	Wed 10/16/02	Wed 4/9/03
Design and Building of Initial Prototypes	36 days	Mon 10/21/02	Tue 12/10/02
Design and Building of Final Prototype	47 days	Fri 2/7/03	Tue 4/15/03
Final Testing	2 days	Thu 4/17/03	Mon 4/21/03

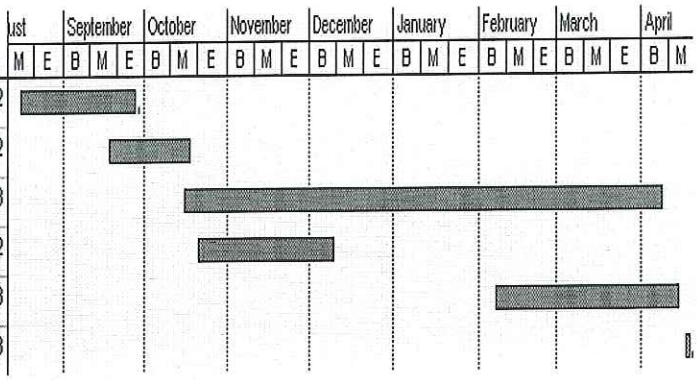

Appendix G: Group Member Contributions

Eric Barta

Eric was responsible for designing and constructing the relief section initial prototype. Once this design was completed, and the tests indicated that a new design would need to be pursued, Eric focused his efforts on debugging the testing setup and brainstorming a new active tether design with Chris Kruzel. Eric spent a large amount of time fabricating parts for this design and was a part of the final testing. Also at the end of the project, Eric investigated the failure of the flexible drive shaft in the powered wheel application. Eric worked on several of the pro-Engineer drawings that were used in this report as well as the final senior design presentation. In addition to these specific tasks, Eric was an integral part of all group reports and projects that were generated throughout the course of the project.

Chris Kruzel

Chris was initially responsible for researching the inspiration for an active tether design. Following this task, he assisted with the construction of the relief section prototype and the powered wheel prototype. Once these designs were abandoned, Chris was in charge of designing the cilia design concept. At the end of the project, Chris focused on construction and debugging the cilia design prototype. In addition to these specific tasks, Chris was an integral part of all group reports and projects that were generated throughout the course of the project.

Mason McIntire

Mason was initially responsible for designing and constructing the powered wheel prototype. Once this was completed, Mason focused his attention on debugging the test setup that had been developed by Laura Wille earlier in the project. Mason developed a new strain gauge setup for measuring the drag of the tether designs and developed the equations necessary for predicting strain as a function of force. Mason worked on several of the pro-Engineer drawings that were used in this report as well as the final senior design presentation. In addition to these specific tasks, Mason was an integral part of all group reports and projects that were generated throughout the course of the project.

Laura Wille

Laura was focused on the testing setup for the majority of the project. She assisted with the development of the original prototypes, but quickly shifted to developing a means of testing the designs. Laura drafted the test plan that would later be used for testing and did the preliminary work in designing the data-acquisition setup. With the assistance of Mason in the second half of the project, this task was successfully completed. In addition to these specific tasks, Laura was an integral part of all group reports and projects that were generated throughout the course of the project.

Appendix H: Success of Design Concepts

1. Establishment of Design Specifications and Criteria:

The design criteria were created by the group in the beginning of the semester. The criteria include reducing the drag places on the robot by the tether. The drag from our active tether should be less than an existing active tether. Next, the tether should be reasonably flexible and able to survive environmental hazards. The tether needs to be transportable and storable as would be necessary in a disaster area. The inner diameter of the tether needs to be big enough so it can carry a range of payloads. Finally, the cost and power consumption should be kept to a minimum. We modified these criteria after the first two prototypes were built. We then said the tether should have a maximum diameter of 2 inches, no rigid sections larger than 1 inch and no more than 3 inches between rigid sections.

2. Analysis:

The analysis of our tether consisted of many tests which were discussed in our report as well as the criteria mentioned above.

3. Synthesis:

The synthesis of this design consisted of taking the concept of cilia and integrating it into a tether. This biological phenomenon gave us the inspiration for movable aluminum rods combined with distinct sections of tether that have the capability of propagating motion.

4. Health and Safety:

The active tether design contains no sharp edges or small detachable parts which can be unsafe. A danger comes from the possibility of the tether pinching. With the distinct sections, it is possible to get body parts caught in the gap and mauled when the tether is moved.

5. Social, Political and Environmental Considerations:

The active tether was designed to increase the mobility of a search and rescue robot in disaster areas. If the idea is implemented, it has the possibility to favorably change the rescue efforts after disasters. Search and rescue robots would be able to go in places they could not previously go and gather much more information about disaster areas. The active tether has a social impact by aiding the performance of the search and rescue robot, which can potentially save more lives. This design addresses the problem of a tethered robot, which can lead to more research and development in the area of search and rescue robots.

6. Construction:

Our design was constructed of many readily available materials such as PVC pipe, aluminum rods, wire rope, and Nomex Aramid. If this design were to be reproduced, these materials could easily be found. The building of the tether is fairly simple due to few parts.

7. Testing:

The testing of our tether consisted of running it through an obstacle course and measuring the drag. Other tests included measuring the volume, length of exposed tether and turn radius. All of these are outlined extensively in the design report.

8. Evaluation:

Many our original design criteria were met. The drag placed on the robot by the active tether decreased in half of the tests compared with the passive tether. The active tether is relatively flexible with a turn radius of only 1 inch greater than the passive tether. The design encloses the tether and only has ¼ inch of exposed tether when bent. There is a threefold increase in volume as compared with the passive tether. This is to be expected when building an encasing for the passive tether. The inner diameter of ¾ inch is large enough to carry a range of payloads. Also, the tether is made out of easily available materials and is relatively inexpensive. Finally, with no motor our tether has no power consumption.

9. Communication:

The group met once a week with our group advisor, in addition to two other group meetings where the advisor was absent. We used blackboard to update the group administrator on weekly progress.

10. Mathematical Modeling:

Mathematical modeling was used in analyzing the strain gauge and to relate the strain to the output voltage of the data acquisition system. A calibration curve was developed for both the Wheatstone bridge as well as the entire data acquisition system.

11. Chemical, Electrical, and Mechanical engineering analogs:

No analogs were used in our design

12. Optimization:

The forward motion angle of the aluminum rods was optimized to allow for a maximum distance between rings of cilia. Optimization was also used to provide enough space between the rigid structure and a flat surface, when two cilia make contact with the surface.

13. Ethics:

The principle of using search and rescue robots to gather information in disaster areas as well as rescuing people is an ethical pursuit.

14. Aesthetics:

The first two prototypes were analyzed aesthetically to see if the designs were practical. We found that due to the size of the designs, it was impractical to pursue a design that was this large and bulky. This analysis allowed us to construct a new set of criteria to which the final design must adhere. The final design was also analyzed aesthetically to find any sharp corners or edges on which somebody could cut themselves.

15. Robust Design:

The final design was constructed from aluminum rods, which have a high tensile strength. The cable to which the rods are attached has a breaking strength of 480 lbs, and the connection that holds the cables in place has a breaking strength of 28 lbs. The maximum force expected on any rod is approximately ten (10) lbs. With a safety factor of two (2), the maximum force is twenty (20) lbs. Therefore, the breaking strength of the connections is 40% above the maximum expected force. Nomex Aramid was placed between each ring of cilia to further protect the tether. Nomex Aramid has a maximum temperature rating of 600°F. The cilia design addresses both extreme temperatures, as well as abrasion from rough surfaces.

16. Economics and Life Cycle Analysis:

The cost of production of 100 ft of the active tether design will cost $1303.83. A length of 100 ft is an approximation of what may be used in a real search and rescue operation. Due to few moving parts, the design is not prone to failure. With routine maintenance and repair, any ring of cilia that is damaged can be easily replaced. Moreover, since the design consists of many rings of the cilia, any one damaged ring will not hinder the performance of the overall design.

17. Manufacturability, Reliability, and Sustainability:

The cilia design can be quickly constructed and assembled due to few parts. All materials used in the cilia design are readily available from hardware stores, as well as from any hardware parts manufacturer that can be found online. The design was constructed and assembled with ease in the Engineering Shop at Trinity University. The only machines needed for construction are the grinding wheel, ban saw, drill press, and a Dremel® tool. Since these tools are available in almost all machine shops, the manufacturability of this design is good.

The design is reliable because there are few moving parts. With a safety factor of 240%, the design is built to withstand unforeseen environments. Moreover, the cilia design uses metal rods to make contact with any obstacles which will perform better than any other material.

With routine inspection, the cilia design is highly sustainable since there are few moving parts. Since each ring of cilia is independent, any one ring can be easily replaced. Therefore, the life of the design is sustainable.

References

{1} C.C. Perry, and Lissner, H.R. The Strain Gage Primer McGraw-Hill, New York 1955.

{2} Wynn, Ryan, "Choosing the Right Strain-Gauge for Your Application";

http://zone.ni.com/devzone/insights.nsf/2d17d611efb58b22862567a9006ffe76/e4d21d414901984486256cb7007115ac?OpenDocument; 4/29/03

{3} "Low Cost, Low Power Instrumentation Amplifier 8620"

http://www.analog.com; 05/01/03

Appendix J: Flexible Drive Shaft Analysis

The results of preliminary flexible drive shaft testing were given in Section 3.1.2 of this report. Following the publication of this report, a more detailed testing analysis has been conducted. The results and analysis from this testing is given below:

Table J1: Flexible Drive Shaft Testing Summary

Bend Radius (in)	Length of Shaft (in)	Orientation	Failure Weight (g)	Failure Torque (in lb)	Notes:
none	18	forward	210	**0.694575**	
none	18	backwards	140	0.46305	2 revolutions before failure
2.5	18	forward	70	0.231525	
2.5	18	backwards	60	0.19845	1 revolution before failure
2.025	18	forward	60	0.19845	
2.025	18	backwards	50	0.165375	
none	12	forward	130	0.429975	
none	12	backwards	100	0.33075	1 revolution before failure
2.5	12	forward	90	0.297675	
2.5	12	backwards	80	0.2646	
2.025	12	forward	70	0.231525	
2.025	12	backwards	45	0.1488375	
none	6	forward	150	0.496125	
none	6	backwards	120	0.3969	
2.5	6	forward	90	0.297675	
2.5	6	backwards	80	0.2646	
2.025	6	forward	60	0.19845	
2.025	6	backwards	50	0.165375	

Table J2: Published Specifications for Flexible Drive Shaft from McMaster Carr (pn# 3135K27)

shaft diameter (in)	max torque (in lb)	min bend radius (in)
0.095	12	2.5

The results of this testing reveals several problems with the application of flexible drive shafts. The most striking problem is that the maximum torque achieved in the testing was 0.695 in lb, while the published specification states that the shaft can transmit 12 in lb. This is a very significant decrease in torque, and as of now, there is no definite explanation for this discrepancy. It is my opinion that a failure of the drive shaft occurs at a very low torque when there is not a rigid casing around the shaft. The flexible drive shaft was free to buckle in this series of testing because there was no casing to prevent it from doing so. It therefore seems to me that in order to transmit the published torque maximum that the drive shaft must be enclosed in a rigid shell. This hypothesis has not been tested, but would be easy to test in the future. This is defiantly a test that someone should conduct before using a flexible drive shaft in future applications.

The testing did however reveal the trends for torque transmission in a variety of drive shaft configurations. The optimal configuration for the maximum torque transmission is no bend radius and a long segment of the flexible drive shaft oriented in the forward direction. Orienting the drive shaft in the wrong direction reduces the torque transmitted by approximately 35%. Additionally, the smaller the bend radius, the lesser the torque transmitted. The most interesting result of the testing is the variance in torque resulting from changes in the shaft length. It appears that there is an optimum length between 9 and 15 inches where the torque transmission is maximized.

Appendix I – How to use the Omega Quadvolt Datalogger

The Omega OM-CP-Quadvolt datalogger contains four voltage inputs. For each input, a reference ground and positive input is needed. The datalogger records voltages either real-time or can be set to record at a later time. The Omega datalogger connects via a USB port to a computer. Omega has its own software on which to set the start time, speed and end time for recording. The fastest recording speed is one data point per second. Recording can last up to nine hours.

The range of the datalogger is -1 to +16 V with a resolution of .5 mV. For more information about this device, refer at the reference manual. This manual can also be found online at http://manuals.omega.com/manualpdf/M3667.pdf.